

We thank all of the reviewers for their valuable comments. Below, we have added some responses (in red) to the comments submitted (in black).

Reviewer 1 Comments:

I have to admit I was a little perplexed at being asked to review this article that really contain no scientific ideas other than the discussion of the experiment and data, but I see from the journal description that is the purpose of this specific journal.

We thank the reviewer for their comments. While ESSD does not field in depth scientific evaluations, it does serve an important purpose in helping to document the data used by the scientific community and help to recognize the work that goes into the collection of such datasets.

The paper describes a unique field campaign and the resulting data obtained. Best I can determine the description of the experiment follows the original motivations, and the document adequately describes the processing performed on the raw data. The data described can be found at the sites identified in the paper, and thus is freely available, although it is not clear to me whether the email request for the TBS data meets the freely available requirement for this journal (I assume it does). Only comment I have is that the authors bring all the labelling in the figures to a standardized format. As is, there is a large degree of variability in font sizes, with some figures nice on the eyes and others with font sizes well below what can be read in print form.

This is a very good suggestion. We have updated our figures to have common font sizes (10 pt), assuming that figures are either 6.5” wide (full page width) or 3” wide (single column width).

Reviewer 2 Comments:

The authors describe measurements and provide sound and unique dataset of the lower Arctic atmosphere obtained at Oliktok Point, Alaska using tethered balloons, unmanned aircraft and radiosondes. Personally, I am not a big fan of do-it-yourself science on the base of provided data sets, but I understand somebody might be. The manuscript reads well and fulfils the requirements of the journal. Also data sets are accessible via ARM Data Management Facility as guided in manuscript and obey common standards. I have not found any flaws in presentation quality of the manuscript. I have only minor comments to current version of the manuscript, please see below.

We would like to thank the reviewer for their time in reading through the manuscript. We have to admit that we don't quite understand the “do-it-yourself science” statement, and it is unclear as to whether it is in response to the material in this paper, or to the potential for someone to use this paper and conduct their own science with the measurements. In either case, as the PIs and executing team for this field campaign, we hope that the measurements are used widely and welcome anyone to access the datasets.

1. Introduction, p3, 189, the following sentence is bit confusing, “. . . and one additional radiosonde per day (three launches daily). . .”. Does it mean at least one per day and/or up to three per day?

This statement meant that one additional radiosonde was launched daily during the campaign (on top of the two that are launched at all times. This results in three launches daily. We have updated the text to read “(three launches daily versus the standard twice-daily launch schedule followed at the observatory)

2.2 DataHawk2 sUAS, p6, 1225, How authors determined the cloud base altitude and how close they operated their sUAS to cloud base, could they be more specific?

We have updated the text to include “as determined from the observatory ceilometer and visual tracking of the aircraft” and “While the cloud base height is variable, ideally the altitude held by the aircraft would be within 25 m of the mean cloudbase level.”

2.5. Overview of completed flights and radiosonde launches, p7, 1280. This is very interesting reading, could authors be bit specific about the distance of take-off area to radar station? Maybe also radar frequency and its power? I understand if authors do not want to share those details, I am just curious.

We have added: “located approximately 150-300 m from the primary DataHawk2 flight areas”. Regarding the frequency and power, we have not included this in the paper because our knowledge is limited to what can be found on Wikipedia. However, we assume this to be a combination of AN/FPS-117 and AN/FPS-124 radar systems from Lockheed Martin. These are D/L-band (1215-1400 MHz) systems that typically operate at 24.6 kW (117) and an unknown power (124).

3. Data processing and quality control, p9, 1359. Authors describe quality control of POPS instrument; however nothing is mentioned about TSI 3007 total aerosol sensor. Also by “flow correction”, p9, 1365, do authors mean flow correction for the height or routine flow calibration at ground level?

There is no correction applied to account for altitude changes. In terms of general quality control, the TSI 3007 is routinely calibrated to ensure that the flow rate is correct, and ground base comparisons are conducted with other butanol CPC to ensure that these are within 15% of one another in terms of particle concentration. Additionally, daily zero count checks are completed, and the alcohol wick is recharged and replaced as needed. Data is flagged as "questionable", when particle concentrations are higher than 10^5 particle/cc, because of a lack of correction for coincident sampling at high concentrations. We have added this material into the body of the text.

Reviewer 3 Comments:

The article provides a good overview of the measurement activities at a very important measurement site. More details on the sensors and data quality would be nice, as specified below.

In particular for the growing community using unmanned aerial systems, more specific descriptions would be helpful. I suggest to perform minor revisions, as suggested in the following, before publishing the manuscript.

- title: “Atmospheric observations” sounds very general. In the overview, mainly meteorological parameters are presented. What about aerosol? There are aerosol sensors, and aerosol measurements have been done. Why is this not included in the overview, and at least some profiles are shown? Are the aerosol data included in the data bases? I would suggest modifying the title to know what is meant by “atmospheric observations”.

We realize that this is a general name but given the fact that we were observing atmospheric thermodynamic state, dynamic state, and aerosol properties, it seemed appropriate to us to have this be wide-ranging. The reviewer makes a good point about not having included enough information on the aerosol measurements. We have added a paragraph in the “overview of completed flights” section on aerosols and added an aerosol-centric figure.

- l. 194: which autopilot was used?

The DataHawk2 uses a custom autopilot developed at the University of Colorado.

- Section 2.2: please specify exact type of each sensor, plus manufacturer and country of origin. This makes it easier for other users to identify the sensor, and do comparisons.

We do not believe that including the country of origin and many details on the sensors will help this paper. While we agree that it is useful to understand what sensor was used and have added some additional details. However, ultimately so much depends on **how** the sensor is integrated, that just having the sensor model number does not necessarily provide useful information to the reader. Therefore, for many readers having exhaustive detail on the sensors would be distracting rather than help to provide insight on the field campaign and the types of measurements that are available.

- l. 223: What is the typical turnaround time between two flights?

Back-to-back flights can be completed with a turnaround time of as little as 10 minutes. Some time is required to change the batteries and re-calibration of the navigation system. We added the following line to the text: “The turnaround time between flights can be as short as 10 minutes, but is generally on the order of 15-30 minutes.”

- l. 237: remove the bracket at the end

Thank you for pointing this out – we have removed the extra parenthesis and period.

- l. 292/ Fig. 6: Please comment on the obvious gaps in the time series of the measurements

As mentioned, the tethered balloon and DataHawk2 were scheduled to operate on alternating two-week time periods over the three-month campaign. As discussed in the text, the DataHawk2

(represented by the red points on the map) was grounded half way into its second deployment due to EMI issues related to the long-range surveillance radar at the site. Therefore, the red dots stop after the middle of the campaign. The DataHawk2 was scheduled to complete a third two-week deployment in early September, which is why there is a large gap there. Gaps in the tethered balloon periods and radiosonde launches were weather-related.

- 1. 412: please show some results of the aerosol and cloud microphysical properties as well

As mentioned above, we have included a figure with aerosol data. The cloud liquid water content data is not tested enough (or processed enough) to include in a figure at the current time. We mention it because there may be people interested in analysis of such a measurement.

- 1. 417: up to which wind speed were radiosonde launches possible?

The ARM program will launch radiosondes in winds up to 30 mph (13.1 m/s). We have added this to the text.

- 1. 440/441: “derivation of wind estimates”, Table 2 – please provide error bars for wind speed!

We have updated this text and have added wind accuracy estimates based on a recent comparison with surface-based instrumentation (Barbieri et al., 2019).

- Table 1 and 2: please use the same style, e.g. with units of accuracy, put the caption either on top or at the bottom of the table, provide at least a conservative estimation on wind speed accuracy

We have updated the tables to have similar styles. Additionally, we have added rough estimates of wind uncertainties based on recent intercomparison work.

- Fig. 4: which temporal resolution of the data is shown? Averaged over 30 min? 1 day?

The temporal resolution shown is one minute. We have added this in the caption.

- Fig. 5: The colour scheme is misleading. I would expect that colours indicate measurement days. What does the colour white mean here? I would mark the flight days, but not the non-flight days. I would further suggest leaving the setup days and the “No UAS/TBS Sampling Scheduled” white, as there were no measurements. The reader should have an overview of data availability, not on other activities. Please explain why you mention in particular the intercomparison days with a C. What does it mean for the data? Is the data better on this day? Was a new calibration performed?

We appreciate this feedback. However, we were trying to distinguish between days when the TBS/DataHawk2 were scheduled to fly but couldn't because of weather (light green) and days when they were not scheduled to fly (white). We agree that the “No UAS/TBS sampling scheduled” dates could be made white as well and have done so in the revised figure. The intercomparison dates were days on which the teams overlapped, and therefore, some priority was given towards surface-based intercomparison of sensors, as well as spatial and temporal co-

location of flights. This resulted in data that can be compared to evaluate whether there are any notable biases between different sensors.

- Fig. 7/8: Please explain the white dot – probably the launch site? Add in the caption that the balloon flight locations are marked in blue, and the DataHawk flights in red.

The white dot is the center of the airspace used. The launch locations varied, but were generally near the AMF-3 (white triangle). We have updated the caption as recommended.

- Fig. 9: Very nice and important plot! It would be good to have some more discussion on it. Could you do something similar for aerosol, of course for lower altitudes only?

We completely agree that the radiosonde data should be explored and discussed in far greater detail, though we believe that such a description would be outside of the scope of an ESSD article (and likely deserves its own article in a journal geared towards scientific analysis of data). We have added a figure for aerosol data from the TBS flights.

Atmospheric observations made at Oliktok Point, Alaska as part of the Profiling at Oliktok Point to Enhance YOPP Experiments (POPEYE) campaign

Gijs de Boer^{1,2}, Darielle Dexheimer³, Fan Mei⁴, John Hubbe⁴, Casey Longbottom³, Peter J. Carroll⁴, Monty Apple³, Lexie Goldberger⁴, David Oaks⁵, Justin Lapierre⁵, Michael Crume⁵, Nathan Bernard⁵, Matthew D. Shupe^{1,2}, Amy Solomon^{1,2}, Janet Intrieri², Dale Lawrence⁶, Abhiram Doddi⁶, Donna J. Holdridge⁷, Michael Hubbell⁴, Mark D. Ivey³, Beat Schmid⁴

- 1) Cooperative Institute for Research in Environmental Sciences, University of Colorado Boulder, Boulder, CO, 80304, USA
- 2) NOAA Physical Sciences Division, Boulder, CO, 80304, USA
- 3) Sandia National Laboratories, Albuquerque, NM, USA
- 4) Pacific Northwest National Laboratory, Richland, WA, USA
- 5) Fairweather, LLC, Anchorage, AK, USA
- 6) Department of Aerospace Engineering, University of Colorado Boulder, Boulder, CO, USA
- 7) Argonne National Laboratory, Lemont, IL, USA

Correspondence to: gijs.deboer@colorado.edu

Abstract. Between 1 July and 30 September 2018, small unmanned aircraft systems (sUAS), tethered balloon systems (TBS), and additional radiosondes were deployed at Oliktok Point, Alaska to measure the atmosphere in support of the second special observing period for the Year of Polar Prediction (YOPP). These measurements, collected as part of the “Profiling at Oliktok Point to Enhance YOPP Experiments” (POPEYE) campaign, targeted quantities related to enhancing our understanding of boundary layer structure, cloud and aerosol properties and surface-atmosphere exchange, and provide extra information for model evaluation and improvement work. Over the three-month campaign, a total of 59 DataHawk2 sUAS flights, 52 TBS flights, and 238 total radiosonde launches were completed as part of POPEYE. The data from these coordinated activities provide a comprehensive three-dimensional data set of the atmospheric state (air temperature, humidity, pressure, and wind), surface skin temperature, aerosol properties, and cloud microphysical information over Oliktok Point. These data sets have been checked for quality and submitted to the US Department of Energy (DOE) Atmospheric Radiation Measurement (ARM) program data archive (<http://www.archive.arm.gov/discovery/>) and are accessible at no cost by all registered users. The primary dataset DOIs are 10.5439/1418259 (DataHawk2 measurements; Atmospheric Radiation Measurement Program, 2016b), 10.5439/1426242 (TBS measurements; Atmospheric Radiation Measurement Program, 2017) and 10.5439/1021460 (radiosonde measurements; Atmospheric Radiation Measurement Program, 2013a).

42 1. Introduction

43 Recent decades have seen notable shifts in Arctic climate (Serreze et al., 2007; Screen and
44 Simmonds, 2010). Reductions in sea ice (Maslanik et al., 2011; Comiso et al., 2008), evident as an
45 integrator of a warming Arctic atmosphere (Dobricic et al., 2016; Graversen et al., 2008), and
46 evolving surface energy budget (Mayer et al., 2016; Hudson et al., 2013) act to enhance
47 absorption of solar radiation at the surface due to a dramatic shift in surface albedo (REFS),
48 potentially enhancing Arctic warming. Sea ice reductions also present opportunities for
49 commerce, including natural resource extraction, shipping, and fishing (Smith and Stephenson,
50 2013; Ho, 2010). Finally, these changes have direct implications on border security due to
51 reduced difficulties with navigation in Arctic waters.

52 In recognition of the importance of these changes and our need to be able to predict and
53 understand them, several nations have established Arctic atmospheric observatories. These
54 observatories measure atmospheric state, cloud properties, aerosols, winds, and surface
55 meteorology, providing critically needed datasets for assimilation into numerical weather
56 prediction models and to advance the physical understanding of the Arctic atmosphere. In
57 northern Alaska, the US Department of Energy (DOE) Atmospheric Radiation Measurement
58 (ARM) Program currently operates two such observatories. The first is the long-term North Slope
59 of Alaska (NSA) site located in Utqiagvik, which has operated since the late 1990s. Additionally,
60 since 2013, the DOE ARM program has operated its third ARM mobile facility (AMF-3) at Oliktok
61 Point, Alaska. Consortia such as the International Arctic Systems for Observing the Atmosphere
62 (IASOA, Uttal et al., 2016) have formed to support the efficient synthesis of measurements from
63 these and other observatories around the Arctic.

64 These observatories only represent a fraction of the work to improve our ability to predict the
65 Arctic environment. Groups such as the World Weather Research Programme (WWRP) Polar
66 Prediction Project (PPP) have developed concentrated efforts to support such work. An example
67 of such an effort is the Year Of Polar Prediction (YOPP), taking place from mid-2017 through mid-
68 2019, which directly targets the improvement of prediction capabilities across a wide variety of
69 time scales, from hours to seasons, through coordinated and intensive observations and focused
70 modeling activities. During the “core phase” of the YOPP, two “special observing periods” (SOPs)
71 were conducted in 2018. This includes one SOP in spring (1 February 2018 to 31 March 2018)
72 and one in late summer (1 July 2018 to 30 September 2018). The “core phase” will be followed
73 by a three-year “consolidation phase”, during which a variety of experiments and analysis
74 projects will leverage the datasets collected during the core phase to evaluate and improve
75 models, conduct data denial experiments, and evaluate the state of polar prediction.

76 Based on the input of the global weather and climate modeling communities, YOPP has
77 established a set of detailed modelling priorities, including:

- 78 • *Boundary layer including mixed phase clouds*
- 79 • *Sea ice modelling*
- 80 • *Physics of coupling, including snow on sea ice*

- *High resolution modelling including ensembles*
- *Model validation and intercomparison*
- *Upper ocean processes*
- *The stratosphere*
- *Chemistry, including aerosols and ozone*

As part of the second SOP, the DOE ARM program supported efforts to enhance observational coverage of the atmosphere at the AMF-3 in Oliktok Point, Alaska (Figure 1). This project, titled “Profiling at Oliktok Point to Enhance YOPP Experiments” (POPEYE) included deployment of the DataHawk2 unmanned aircraft system, tethered balloon systems, and one additional radiosonde per day (three launches daily versus the standard twice-daily launch schedule followed at the observatory) to provide measurements needed to help meet the objectives above. The lower-atmospheric thermodynamic observations offer a detailed look into the Arctic summer time boundary layer providing insight into its structure and evolution, and a means of validating retrieval algorithms from remote sensors. Such measurements support the stated YOPP goal of pursuing an integrated modeling framework to connect cloud, boundary layer and surface energy exchange schemes through Large Eddy Simulation (LES)-based development. Additionally, POPEYE provides a detailed dataset that can be used for evaluation of model performance across a variety of model products (e.g., reanalyses, weather forecast models, coupled regional forecast models, global climate models), and more frequent radiosondes can help assess the impact of data assimilation on operational models. This facilitates studies on the impact of enhanced Arctic observations on predictions of lower latitude weather (e.g., Jung, 2014; Inoue et al. 2015). The measurements collected can also provide constraints on the initial and boundary conditions for intercomparisons of single-column and large eddy simulation models. The increased frequency of radiosonde launches provides an enhanced look into the Arctic stratosphere, further supported by the launch of additional radiosondes at other observatories during this SOP. Finally, POPEYE aerosol measurements provide information on the vertical structure of key particle properties.

Deleted: three launches daily

This paper describes the dataset collected during POPEYE. Section two includes information on the systems and sensors used, sampling strategies employed, limitations related to weather and other factors, and a general overview of the dataset as collected. Section three provides background on the data processing and quality control measures applied to the datasets collected during POPEYE, and information on the different levels of data resulting from this effort. Section four provides information on the availability of the data, including a link for where the datasets can be downloaded. Finally, section five provides a summary of the POPEYE campaign.

2. Description of Measurements and Sampling Strategy

POPEYE featured a focused deployment of three observational tools during the second northern hemispheric YOPP SOP. These measurements were designed to complement measurements from the instruments integrated into the AMF-3, which run continuously and are therefore not described in detail in this paper. The reader is referred to comprehensive information available through the ARM web page (www.arm.gov). The three datasets described here are those that

were specifically deployed as a part of POPEYE, including the DataHawk2 small unmanned aircraft system (sUAS), two tethered balloon systems (TBSs) and extra radiosondes. All systems were deployed by DOE ARM operators, and the Datahawk2 and TBS systems have been deployed regularly at Oliktok Point over the past few years (de Boer et al., 2018). Here we provide information on these systems and the sensors operated on each.

2.1. Tethered Balloon Systems

TBSs mainly consisted of two different balloons, a 35 m³ helikite constructed by Allsopp Helikites and a 79 m³ aerostat constructed by SkyDoc™. The helikite is a balloon/kite hybrid that uses lighter-than-air principles to obtain its initial lift, and a kite to achieve stability and dynamic lift, while the larger aerostat uses a skirt instead of a kite to achieve stability in flight. Lift of both a helikite and an aerostat increase with increasing wind speed, so a relatively stable float altitude can be achieved even in elevated wind speeds. For POPEYE operations, both systems were operated using an electric winch integrated into a dedicated balloon trailer by Sandia National Laboratories. The payload and operating guidelines for the TBSs vary significantly with location and environmental conditions. Generally, the aerostat is operated for total payload weights of 8 – 27 kg, and the helikite is operated for total payload weights < 27 kg. The helikite is not typically operated above 600 m AGL, because beyond this altitude the weight of the tether and payload exceed the maximum lifting force of the helikite. The aerostat can be operated at higher altitudes, but due to its larger size is not launched in sustained surface wind speeds > 7 m s⁻¹. The helikite is not launched in sustained surface wind speeds > 11 m s⁻¹. Operation of either platform is suspended, and the balloon is immediately retrieved if sustained wind speeds at the altitude of the balloon exceed 15 m s⁻¹. In general, the strength of the wind is the main limiting factor governing the launch and final altitude of the TBSs, with rime accretion on the tether, instruments and balloon also contributing to altitude limitations.

POPEYE TBS operations involved a variety of sensors and payloads. To measure the thermodynamic properties of the atmosphere, the TBS team operated multiple different sensor packages from interMet. This includes the interMet iMet-1-RSB radiosonde package as well as the interMet XQ2 sensor packages developed for use on UAS. Additionally, a Silixa XT distributed temperature sensing (DTS) system was flown. This system, which includes a long fiberoptic cable suspended along the tether, provides a high resolution, continuous measurement of air temperature based on Raman scattering (Keller et al. 2011; DeJong et al. 2015). Using this system, the temperature is typically measured along the length of the optical fiber every 30 to 60 seconds at 0.65 cm spatial resolution. To provide information on the winds aloft, vane cup anemometers from APRS World were operated at specified intervals along the tether. It is important to note that while wind speed from these sensors appears to be relatively accurate when compared with Doppler lidar measurements, a variety of factors including the high latitude location make the directional measurement inaccurate. Information on the aerosol particle population was provided using a combination of two Handix Scientific Printed Optical Particle Spectrometers (POPS) and a TSI Condensation Particle Counter (CPC) 3007. The two POPS provide information on the aerosol size distribution for particles between 140-3000 nm while the CPC provides information on the total number of particles between 10-1000 nm. Additionally,

vibrating wire sensors from Anasphere and the University of Reading provide information on the amount of supercooled liquid water in cloud. These sensors were collectively referred to as “Supercooled Liquid Water Content” (SLWC) sensors. Further details on all of these sensors and the expected level of accuracy (where available) are included in Table 1.

The main role of the TBS in POPEYE was to collect detailed information on the vertical structure of the lower atmosphere over the AMF-3. This provides information on stratification and the temporal evolution of the lower atmospheric structure. Additionally, the TBS is unique in that it is able to fly in and above cloud for extended time periods, providing an opportunity to collect in-situ measurements of thermodynamic, aerosol and cloud microphysical properties on low-altitude Arctic clouds. To accomplish this, the TBS was flown as high as weather conditions would permit, conducting repeated profiles with sensors distributed along the tether. While the exact placement of the sensors would change from flight to flight to adapt to the present conditions, in general the system was operated with a cluster of sensors including a POPS, CPC, iMet and SLWC near the top of the tether under the balloon, a DTS fiber along the entire length of the tether, and subsequent iMet sensors and anemometers below the main package as most desirable based on the meteorological conditions. When flying the aerostat, a second POPS would also be flown to get more detailed measurements of evolution of the aerosol profile in time. A schematic outlining this strategy is included in Figure 2.

2.2. DataHawk2 sUAS

Another instrument platform used during POPEYE was the Datahawk2 sUAS, developed at the University of Colorado Boulder (description of the first version of the DataHawk can be found in Lawrence and Balsley, 2013). The DataHawk2 sUAS is a small (1.2 m wingspan, <1 kg take-off weight), robotic, pusher-prop aircraft designed to operate in a variety of conditions as a flexible and inexpensive measurement platform (see Table 2 for the specifications of the DataHawk2 UAS). The DataHawk2 has been used for a variety of purposes, including the study of turbulence (e.g. Kantha et al., 2017; Balsley et al., 2018) and high latitude (e.g. de Boer et al., 2016; 2018) deployments. The relatively slow flight speed (14 m/s, burst up to 22 m/s) allows the platform to obtain measurements at high spatial resolution when compared to other aerial vehicles. Despite this relatively slow speed, the DataHawk2 has been operated in winds up to 12 m/s, making it a robust research platform for the harsh Arctic environment. DataHawk2 flights completed under POPEYE were generally autopilot guided except for during take-off and landing, when they were under the control of a local pilot through real-time telemetry. All flights were completed within radio communication range and within sight of the ground operators and were conducted within restricted airspace (R-2204, see Figure 1, de Boer et al., 2016) controlled by the US DOE. This allowed operators to adjust the flight plan in real time to meet the needs of the science objectives and adapt to the changing environment. The ground controller and UAS communicate via 2.4 GHz radio with a range of approximately 10 km. Regulations limit DataHawk2 flight to within visual line of sight, meaning that it is not allowed to fly into clouds and follow VFR weather minimums for operation (14 CFR 91.155). Additionally, winds hamper the operation of the DataHawk2, with DOE ARM guidelines restricting flight when winds top 7 m s⁻¹.

207 The DataHawk2 carries a variety of sensors to make measurements of the atmospheric and
208 surface states. Custom-built instrumentation includes a fine wire sensor employing two cold- and
209 one hot-wire. These provide high-frequency (800 Hz) information on temperature and fine scale
210 turbulence. High bandwidth is enabled by small surface-area-to-volume ratios of very thin (5 µm
211 diameter) wires. In addition, the DataHawk2 carries a custom configuration that includes
212 integrated-circuit slow response sensors (Sensiron SHT-31) for measurement of temperature
213 through a calibrated semiconductor, and relative humidity using a capacitive sensor. For POPEYE
214 specifically, the DataHawk2 also carried an E+E EE03 digital temperature and humidity
215 (capacitive) sensor that was externally mounted on the airframe. For information on surface and
216 sky temperatures, DataHawk2s are equipped with up- and downward-looking thermopile sensors
217 (Semitec 10TP583T with custom electronics). These sensors undergo a calibration using targets
218 of a known temperature. Finally, DataHawk2s have also carried the commercially-available iMet1
219 radiosonde package, providing comparative information on position (GPS), temperature (bead
220 thermistor), pressure (piezoresistive) and relative humidity (capacitive), though these sensors
221 were not installed during POPEYE.

222 The main objective for the DataHawk2 was to obtain as many profiles as possible of the lower
223 atmosphere during daytime hours. To do this, the aircraft was programed to climb from the
224 surface to the maximum obtainable altitude. This maximum altitude was constrained by the
225 pilot's ability to maintain visual contact with the aircraft (1000 m AGL) or by the cloud ceiling.
226 Because the endurance of the aircraft is approximately 50 minutes in Arctic operating conditions,
227 the aircraft could generally complete between one and two full profiles before needing to land
228 to change batteries. The turnaround time between flights can be as short as 10 minutes, but is
229 generally on the order of 15-30 minutes. Because of the substantial interest in the interplay
230 between thermodynamic and dynamic properties near cloud base, during cloudy conditions, the
231 operators were requested to hold altitude around the cloud base height, as determined from the
232 observatory ceilometer and visual tracking of the aircraft, for 10-15 minutes to collect statistics
233 of that environment before descending back towards the surface. While the cloud base height
234 is variable, ideally the altitude held by the aircraft would be within 25 m of the mean cloudbase
235 level. Figure 3 provides an illustration outlining this flight pattern.

237 2.3. Radiosondes

238 The DOE ARM program launched Vaisala RS-92 radiosondes on a regular schedule under POPEYE.
239 Due to concerns about operator safety and fatigue, the number of radiosondes launched was
240 scheduled at three per day, with requested launch times of 05:30, 17:30 and 23:30 UTC (21:30,
241 09:30, 15:30 AKDT) to match the 06:00, 18:00 and 00:00 UTC synoptic times. Radiosonde
242 launches were at times suspended due to dangerous conditions, including the presence of bears
243 on site, or high winds ($>13.5 \text{ m s}^{-1}$ sustained and gusting $>18 \text{ m s}^{-1}$) which could result in damage
244 to the sensor package if the balloon does not achieve enough vertical lift due to the strong cross
245 wind. Radiosondes are lifted using 350g balloons with an average ascent rate target of 5.5 ms^{-1} .
246 Radiosonde data from the campaign are available through the ARM data archive (Atmospheric
247 Radiation Measurement program, 2013a).

249 2.4. Overview of meteorological conditions sampled

Formatted: Normal

Formatted: Not Highlight

Formatted: Font: (Default) Calibri, 12 pt

Formatted: Font: (Default) Times New Roman, Font color: Auto

Deleted:

Deleted:).

The presence of the ARM AMF-3, allows us to put the measurements from the radiosondes, TBS and UAS in broader context. Figure 4 shows measurements from the AMF-3 surface meteorological instrumentation (Atmospheric Radiation Measurement Program, 2013b) over the three-month POPEYE period. Synoptically, this period featured several driving features. For much of the campaign, there was a stationary area of high pressure positioned over the Gulf of Alaska, and Oliktok Point sat on the gradient between this area of high pressure and transient low pressure systems moving through the Chukchi and Beaufort Seas. This generally resulted in west-northwesterly winds during this time period. Some of these cyclones passed closer to shore, thereby directly impacting the Oliktok Point area and creating precipitation events and shifting wind regimes (e.g. July 7-10; August 13; August 16-17; August 29-31). In late August there was a general shift in the pattern with high pressure beginning to set up over northern Alaska and eventually over the Beaufort Sea to the north. This resulted in a general shift towards easterly winds at the surface. The end of the POPEYE campaign featured a dominant area of high pressure over the area, resulting in weak easterly winds.

Considering the vertical structure of the lower atmosphere, the observations included measurements from a variety of stability regimes. While the presence of the sun in summer months generally results in more adiabatic lower atmospheric states than during other times of year in the Arctic, the data collected indicates sampling of both well-mixed and stratified conditions. This includes several stable boundary layer cases. Additionally, many of the completed flights were flown with some level of cloud cover in place. While the UAS did not sample through the cloud, the TBS was able to do so, providing insight into the thermodynamic and microphysical structure in and around these clouds. Based on ceilometer data from the AMF-3 (Atmospheric Radiation Measurement Program 2013c), a cloud base was detected during 76% of the campaign period. Of the times when clouds were detected, 73% of the cloud bases occurred below 1 km altitude, 21% occurred between 1-4 km altitude, and 6% were found above 4 km.

In general, it is relevant and important to note that to some extent all of the POPEYE platforms were weather-limited in terms of their operations. Therefore, there is an element of selective sampling to consider when using the collected datasets. Most directly, the TBS and UAS systems were generally not operated during high winds. The UAS additionally had limitations related to visibility. The radiosondes were least impacted, though high winds did also prevent some launches.

2.5. Overview of completed flights and radiosonde launches

Over the three-month period, there were limited data outages and challenges related to the issues discussed in the previous sections. Figure 5 illustrates the operations completed under POPEYE. The most significant challenge to continuous operations was the electromagnetic interference (EMI) caused by a US Air Force radar station at Oliktok Point, located approximately 150-300 m from the DataHawk2 flight areas. Modifications made to this radar during the POPEYE time window unfortunately resulted in the grounding of the DataHawk2s for their planned second and third deployments. Additionally, this EMI resulted in some resets of the TBS instrumentation, and errors in the TBS GPS readings. In addition, there were some challenges

296 associated with the Arctic weather. Despite it being summer, winds were a challenge to both
297 TBS and UAS flights at times, and also resulted in the cancellation of some radiosonde launches.
298 Wildlife also posed challenges, as the site is visited by both brown and polar bears during the
299 summer months. The local presence of these large creatures generally required that operators
300 ceased outdoor operations, impacting all three measurement platforms. Despite these
301 challenges, the campaign totaled 238 radiosondes launched, 52 TBS flights (134.3 flight hours),
302 and 59 DataHawk2 flights (64.6 flight hours). Figure 6 illustrates the completed flights in time-
303 height space.

304
305 A map indicating the horizontal extent of the TBS flights is shown in Figure 7 (top). The horizontal
306 distances covered are governed by the positioning of the winch trailer for the system, the wind
307 speed, and the amount of tether extended. The points drifting over the ocean surface are the
308 result of erroneous GPS data, likely linked to EMI from the USAF radar system. The distribution
309 balloon altitudes (the highest sampling height for any given TBS operation) is shown in Figure 7
310 (bottom) and demonstrates that the balloon typically sampled the lowest 1 km of the
311 atmosphere. Because the balloon can hover at a given altitude for extended time periods, there
312 are multiple peaks in the altitude distribution, notably at around 150 m, 300 m, 700 m and 1000
313 m. These altitudes correspond to altitudes chosen for extended sampling during the campaign.
314 Also, a comparison of TBS altitudes with ceilometer-based cloud base measurements indicates
315 that the TBS was operating at or above the lowest detected cloud base altitude 32% of the time.
316

317 A map of the horizontal extent of the DataHawk2 flights is shown in Figure 8 (top). All flights
318 were conducted in close proximity to the AMF-3 instrumentation, within the restricted airspace
319 outlined under R-2204. The flight patterns consisted of profiling of the lowest 1 km of the
320 atmosphere, as indicated by the probability distribution of altitudes sampled in the lower panel.
321 This distribution is binned by 20 m increments and based on this it becomes clear that most
322 common altitude was between 20-40 m above ground level (AGL). From this altitude, the
323 frequency of visiting higher altitudes generally decreases slowly, resulting from limitations
324 imparted by visibility and winds.
325

326 Figure 9 provides insight into the statistics of the radiosonde measurements. The right panel
327 indicates the distance away from Oliktok Point that radiosondes traveled over the length of the
328 POPEYE campaign. Within the troposphere (<10 km altitude), radiosondes generally remained
329 within 20 km of the Oliktok Point facility. However, a few balloons traveled as far as 100 km away
330 once in the stratosphere, with most staying within 50 km of the site all the way to the top of the
331 profile. The temperature-height histogram (figure 6, left panel) reveals a general cooling of the
332 air with height through the depth of the troposphere, with most profiles cooling from
333 temperatures of 0-10 C near the surface to around -50 C at the tropopause. Additionally, there
334 are indicators of frequent low-level inversions in the lowest 1-2 km. There appear to be two
335 modes of temperatures observed in the stratosphere, with a dominant mode between -40 and -
336 50 C, and a secondary mode at around -55 C. Finally, a two-dimensional histogram of the winds
337 with height (Figure 6, middle panel) illustrates a broad range of measurements near the surface
338 (0-20 m s⁻¹), with winds generally increasing with height through the troposphere to values
339 ranging between 5-50 m s⁻¹. Winds in the stratosphere again decrease to less than 10 m s⁻¹.

Figure 10 illustrates time-height cross sections of radiosonde measurements of temperature, relative humidity and wind speed for the duration of POPEYE.

Finally, Figure 11 provides an initial glimpse into measurements from the POPS sensor on the TBS. The top panel illustrates the cumulative number concentrations sampled, showing that the range of particle numbers measured tended to decrease with height, and that higher concentrations were typically sampled in the lowest parts of the atmosphere. This is likely a result of the numerous near-surface sources associated with oil production facilities in the vicinity of Oliktok Point. Additionally, there is some level of contamination very close to the surface from the diesel generator used to run the TBS winch system. The extent of this contamination is a function of wind speed and atmospheric mixing state and cannot be generally quantified. The second panel shows a similar two-dimensional histogram for particle sizes. This figure illustrates that most particles sampled were around 200 nm and that the balloon typically operated below 500 m. Again, the spread of diameters measured appears to increase with decreasing height. For both of the top panels it is important to keep in mind that white areas do not necessarily mean that zero samples were observed in that bin, as the lowest colorbar bin has some finite edges. The bottom panel shows the relationship between particle size and concentration as a function of altitude as observed over the campaign. There are numerous near-surface (dark blue) points where high concentrations of smaller particles were observed. These observations are complimented by measurements from the CPC for the majority of campaign flights (not shown).

3. Data processing and quality control

The US DOE ARM program handles all data collection, quality control, and processing for field campaigns. In general, several different levels of ARM data are made available, ranging from raw data as recorded by the sensors (a-level), to quality-controlled data (b-level) and data products (c-level). This section provides an overview of the processing and quality control applied to the data streams coming from the platforms deployed during POPEYE.

For the DataHawk, current processing techniques provide both raw and processed datafiles. Aircraft performance and sensor data are gathered and stored in a binary format on the onboard SD card. This binary format data is the raw data that is archived by ARM (a0 level). Typically, this raw data is invisible to the community user, but can be requested through the ARM data discovery tool if desired. In addition, the data on the SD card is unpacked, downsampled to 10 Hz, and assigned to a relevant array of variable names, and then exported to NetCDF format as a processed raw data file (a1 level). This data file includes data gathered by onboard sensors during flight, aircraft performance data, telemetry data and GPS data. The next file that is produced is a 10 Hz quality-controlled file that includes some initial conversions (b1 level). For example, raw sensor data from the cold wire sensor and onboard temperature sensors are used to convert the voltage reported by the cold wire into a temperature value. Additionally, relative humidity and infrared temperature values measured are calibrated and converted from the engineering to relevant physical units. Wind components are reconstructed using corrected pitot airspeed data, GPS data, and the aircraft principle axis data to produce wind speed and direction and the three wind components. Finally, a quality control step is applied to remove any significant spikes in the dataset. This quality-controlled dataset is the current final ARM data product for DataHawk2. An

383 additional higher frequency data product is under development for future release, which will
384 provide the turbulence parameters as a value added product (VAP).
385

386 Most of the TBS measurements undergo a similar processing and quality control procedure. In
387 particular, several quality control measures are implemented on the POPS instrument. Included
388 in this processing is a size correction that is determined through routine size checks and
389 calibration. For the size check, 500 nm polystyrene latex (PSL) particles are generated to evaluate
390 the signal response from the POPS instrument and confirm that the instrument performance is
391 steady over the course of the campaign. For the calibration, eight different PSL particle sizes are
392 used to determine the relationship between the optical response signal and particle size. In
393 addition, a flow correction is applied, which is based on routine checks using a flow meter. For
394 the CPC, routine calibrations are conducted to ensure that the flow rate is correct. Additionally,
395 ground-based comparisons are conducted with other butanol CPCs to ensure that measured
396 particle concentrations are within 15% of one another. Also, daily zero count checks are
397 completed, and the alcohol wick is recharged and replaced as needed while the instrument is
398 deployed to the field. Finally, CPC data are flagged as "questionable" when particle
399 concentrations are higher than 10^5 cm^{-3} , because of a lack of correction for coincident sampling
400 at high concentrations.

401
402 Radiosonde data are processed as quality-controlled measurements, with quality control being
403 completed proprietary Vaisala software that corrects for sensor response time and solar
404 radiation exposure.
405

406 4. Data Availability

407 The data files from POPEYE observations are available for public download through the US DOE
408 ARM Program Data Archive (<http://www.archive.arm.gov/discovery/>). ARM uses NetCDF as the
409 standard data file format, with self-describing metadata provided to the user inside the NetCDF
410 file. The data are posted as individual datastreams on the archive, which is searchable by site (in
411 this case OLI for Oliktok Point) and instrument (in this case "TBS" for the tethered balloons,
412 "aafdatahawk" for the DataHawk2, and "sonde" for the radiosondes). Each instrument may have
413 several different levels of data available.

414 The main TBS datastream for measurements from the iMet instruments and basic information
415 on aerosol instrumentation is *olitbsimetM1.a1* (DOI: 10.5439/1246367). ARM is currently
416 working to produce a quality-controlled b1 product. Data from the DTS system has been
417 collected by the ARM Data Management Facility (DMF), and can be requested by email to
418 armarchive@ornl.gov, with the appropriate DTS datastreams for POPEYE being *tbsdtssxforjch1*,
419 *tbsdtssxforjch2*, *tbsdtssxch1*, *tbsdtssxch2*. SLW sensor data is available through the ARM archive
420 under the *tbsslwc.b0* datastream, while the TBS aerosol instrumentation can also be downloaded
421 through the archive as *tbscpcM1.00*, *tbspopdryM1.00*, *tbspopwetM1.00*. All of these datasets
422 are currently provided at 1 Hz. TBS ground station data, including temperature, humidity,
423 pressure and winds at the surface, are available as b-level files on the archive under the file prefix
424 "olitbsgroundM1" as 10-minute average values.
425

Formatted: Superscript

Formatted: Superscript

426 Quality-controlled DataHawk data can be downloaded as *oliaafdatahawkm1.b1* (DOI:
427 10.5439/1426242). Finally, the POPEYE radiosonde dataset is available as a QC'd b1 dataset, with
428 the filenames being of the general form *olisondewnpnM1.b1* (DOI: 10.5439/1021460), where
429 *wnpn* refers to the mode of the sonde data collection. Here, "w"=winds, "p"=PTU (pressure,
430 temperature, humidity), and "n"=nominal indicates a normal flight with data collection during
431 ascent only.

432
433 To make it possible for scientists to cite DOE ARM program data in their publications, ARM
434 recognizes the value of Digital Object Identifiers (DOIs). Such DOIs are generally being generated
435 at the ARM data product level. Data products produced from the a-level data may have their
436 own DOI -- for example, separate DOIs are assigned to each of the available output datastreams
437 and any value-added products (VAP) from the radiosonde measurements obtained by ARM. This
438 means that it is possible that POPEYE measurements could be spread across a variety of DOIs,
439 and that additional DOIs could be created that include POPEYE data as additional data products
440 are developed.

441 5. Summary

442 Between 1 July and 30 September 2018, the POPEYE measurement team collected detailed
443 measurements of the lower Arctic atmosphere at Oliktok Point, Alaska using tethered balloons,
444 unmanned aircraft and radiosondes. This activity resulted in the completion of 134.3 TBS flight
445 hours, 64.6 sUAS flight hours, and 238 radiosonde launches. The primary focus of POPEYE was
446 to provide detailed measurements of the lower atmosphere, including thermodynamic state,
447 aerosol properties, cloud microphysical properties, winds, and surface temperature. UAS flights
448 covered the atmosphere between the surface and 1 km altitude but were unfortunately called-
449 off early due to EMI from the nearby long-range surveillance radar system operated by the US
450 Air Force. Tethered balloon measurements went as high as 1396 m using two different balloons.
451 Radiosondes were launched at a frequency of three times daily, except when environmental
452 conditions (winds $> 13.1 \text{ m s}^{-1}$, bears) prevented balloon launches. These datasets provide a
453 detailed look into processes in the lower atmosphere and set the stage for detailed evaluation of
454 numerical models and, together with ongoing, continuous measurements from the AMF-3,
455 support the development of modeling case studies for process understanding and evaluation of
456 parameterization performance.

457 Quality-controlled versions of the data collected as a part of POPEYE are available on the US DOE
458 ARM data archive. This archive is publicly accessible and allows users to download data from
459 these platforms and all other ARM-operated instrumentation, including measurements from the
460 AMF-3 deployment at Oliktok Point.

461 462 Author Contributions

463 GdB designed the field campaign, acted as principal investigator for POPEYE, conducted field
464 work as part of POPEYE, and led the development of the manuscript. DD, CL and MA were the
465 primary TBS operators during POPEYE, contributed to the processing of TBS data, and contributed

Formatted: Superscript

466 to the writing and review of the manuscript. JH, PC, and LG were the primary DataHawk2
467 operators during POPEYE and contributed to the processing of DataHawk2 data and the writing
468 and review of the manuscript. DO, JL, MC and NB are site operators at Oliktok Point and
469 conducted the radiosonde launches, contributed to site operations during POPEYE and assisted
470 the DataHawk2 and TBS teams while in the field. FM is the instrument mentor for TBS aerosol
471 instrumentation as well as for the DataHawk2 and contributed to data preparation and
472 processing for POPEYE as well as manuscript writing and review. MS, AS, and JI are POPEYE Co-
473 Pls and contributed to campaign planning, field work, and oversight as well as the writing and
474 review of this manuscript. DL is the primary DataHawk2 developer and contributed to the
475 development and review of the DataHawk2 dataset. AD helped with the development of wind
476 estimation techniques using the DataHawk2. DH is the ARM instrument mentor for the
477 radiosondes and contributed to the processing of the radiosonde dataset as well as the writing
478 and review of this manuscript. Finally, MI and BS manage the teams responsible for operation of
479 the TBS and DataHawk2. Additionally, MI is the primary site manager at the AMF-3. They both
480 oversaw and supported campaign activities and additionally contributed to the review of this
481 manuscript.

482 483 Acknowledgments

484 This work was supported by the US Department of Energy Atmospheric Radiation Measurement
485 Program. Support for campaign planning and execution was provided by the US DOE
486 Atmospheric System Research Program under project DE-SC0013306. Finally, additional support
487 was provided by the NOAA Physical Sciences Division. We would like to thank the US Air Force
488 for providing access to the Oliktok Point facility, ENI Petroleum who supported our teams at their
489 Nikaichuq Operations Center, and ConocoPhillips who housed team members at the Kuparuk
490 camp. Finally, POPEYE is an officially-endorsed contribution to the Year of Polar Prediction
491 (YOPP), a flagship activity of the Polar Prediction Project (PPP), initiated by the World Weather
492 Research Programme (WWRP) of the World Meteorological Organisation (WMO). We
493 acknowledge the WMO WWRP for its role in coordinating this international research activity.

494

495 496 References

497 Atmospheric Radiation Measurement (ARM) user facility. Updated hourly. Balloon-Borne
498 Sounding System (SONDEWNP). **2018-07-01 to 2018-10-01, ARM Mobile Facility (OLI)**
499 **Oliktok Point, Alaska; AMF3 (M1)**. Compiled by D. Holdridge, J. Kyrouac and R. Coulter. ARM
500 Data Center. Data set accessed **2018-11-08** at <http://dx.doi.org/10.5439/1021460>, 2013a.
501 Atmospheric Radiation Measurement (ARM) user facility. Updated hourly. Surface
502 Meteorological Instrumentation (MET). **2018-07-01 to 2018-10-01, ARM Mobile Facility**
503 **(OLI) Oliktok Point, Alaska; AMF3 (M1)**. Compiled by D. Holdridge and J. Kyrouac. ARM Data
504 Center. Data set accessed **2018-11-08** at <http://dx.doi.org/10.5439/1025220>, 2013b
505 Atmospheric Radiation Measurement (ARM) user facility. Updated hourly. Ceilometer
506 (CEIL). **2018-07-01 to 2018-10-01, ARM Mobile Facility (OLI) Oliktok Point, Alaska; AMF3**

Deleted: derivation

Deleted: estimates

Deleted: from

510 (M1). Compiled by B. Ermold and V. Morris. ARM Data Center. Data set accessed **2018-11-**
 511 **08** at <http://dx.doi.org/10.5439/1181954>, 2013c.
 512 Atmospheric Radiation Measurement (ARM) user facility. Updated hourly. Tethered Balloon
 513 System (TBSGROUND). **2018-07-01 to 2018-10-01, ARM Mobile Facility (OLI) Oliktok Point,**
 514 **Alaska; AMF3 (M1).** Compiled by D. Dexheimer and Y. Shi. ARM Data Center. Data set
 515 accessed **2018-11-16** at <http://dx.doi.org/10.5439/1246367>, 2016a.
 516 Atmospheric Radiation Measurement (ARM) user facility. Updated hourly. Tethered Balloon
 517 System (TBSIMET). 2017-04-09 to 2018-09-28, ARM Mobile Facility (OLI) Oliktok Point, Alaska;
 518 AMF3 (M1). Compiled by D. Dexheimer and Y. Shi. ARM Data Center. Data set accessed 2019-
 519 03-11 at <http://dx.doi.org/10.5439/1426242>, 2017.
 520 Atmospheric Radiation Measurement (ARM) user facility. Updated hourly. Meteorological
 521 Instrumentation aboard Aircraft (AAFDATAHAWKMET). 2016-06-06 to 2018-08-07, ARM
 522 Mobile Facility (OLI) DataHawk Unmanned Aerial System (U1). Compiled by F. Mei and J.
 523 Hubbe. ARM Data Center. Data set accessed 2019-03-11 at
 524 <http://dx.doi.org/10.5439/1418259>, 2016b.
 525 Balsley, B.B., Lawrence, D.A., Fritts, D.C., Wang, L., Wan, K., and Werne, J.: Fine Structure,
 526 Instabilities, and Turbulence in the Lower Atmosphere: High-Resolution In Situ Slant-Path
 527 Measurements with the DataHawk UAV and Comparisons with Numerical Modeling. *J.*
 528 *Atmos. Oceanic Technol.*, **35**, 619–642, <https://doi.org/10.1175/JTECH-D-16-0037.1>, 2018.
 529 Comiso, J.C., Parkinson, C.L., Gersten, R. and Stock, L.: Accelerated decline in the Arctic sea ice
 530 cover, *Geophys. Res. Lett.*, **35**, L01703, 2008.
 531 de Boer, G., Ivey, M.D., Schmid, B., Lawrence, D., Dexheimer, D., Mei, F., Hubbe, J., Hardesty,
 532 J.O.E., Bendure, A., Shupe, M.D., McComiskey, A., Telg, H., Schmitt, C., Matrosov, S., Brooks,
 533 I., Creamean, J.M., Solomon, A., Turner, D.D., Williams, C., Maahn, M., Argrow, B., Palo, S.,
 534 Long, C.N., Gao, R.-S. and Mather, J.: A Bird's Eye View: Development of an Operational ARM
 535 Unmanned Aerial Systems Capability for Atmospheric Research in Arctic Alaska, *Bull. Amer.*
 536 *Meteor. Soc.*, **99**, 1197-1212, <https://doi.org/10.1175/BAMS-D-17-0156.1>, 2018.
 537 de Boer, G., Ivey, M.D., Schmid, B., McFarlane, S. and Petty, R.: Unmanned platforms monitor the
 538 Arctic atmosphere, *EOS*, **97**, doi:10.1029/2016EO046441, 2016.
 539 Dobricic, S., Vignati, E. and Russo, S.: Large-scale atmospheric warming in winter and the Arctic
 540 sea ice retreat, *J. Clim.*, **29**, 2869-2888, 2016.
 541 Graverson, R.G., Mauritsen, T., Tjernström, M., Källén, E. and Svensson, G.: Vertical structure of
 542 recent Arctic warming, *Nature*, **451**, 53-56, 2008.
 543 Ho, J.: The implications of Arctic sea ice decline on shipping, *Marine Pol.*, **34**, 713-715, 2010.
 544 Hudson, S.R., Granskog, M.A., Sundfjord, A., Randelhoff, A., Renner, A.H.H. and Divine, D.V.:
 545 Energy budget of first-year Arctic sea ice in advanced stages of melt, *Geophys. Res. Lett.*, **40**,
 546 2679-2683, 2013.
 547 Inoue, J., Yamazaki, A., Ono, J., Dethloff, K., Maturilli, M., Neuber, R., Edwards, P. and Yamaguchi,
 548 H.: Additional Arctic observations improve weather and sea-ice forecasts for the Northern
 549 Sea Route, *Sci. Report.*, **5**, 16868, 2015.
 550 Jung, T., Kasper, M.A., Semmler, T. and Serrar, S.: Arctic influence on sub-seasonal midlatitude
 551 prediction, *Geophys. Res. Lett.*, **41**, 3676-3680, 2014.

552 Kantha, L., Lawrence, D., Luce, H., Hashiguchi, H., Tsuda, T., Wilson, R., Mixa, T. and Yabuki, M.:
 553 Shigaraki UAV-Radar Experiment (ShUREX): overview of the campaign with some preliminary
 554 results, *Prog. Earth. Planet. Sci.*, **4**, 19, 2017.
 555 Lawrence, D.A. and Balsley, B.B.: High-Resolution Atmospheric Sensing of Multiple Atmospheric
 556 Variables Using the DataHawk Small Airborne Measurement System. *J. Atmos. Oceanic*
 557 *Technol.*, **30**, 2352–2366, <https://doi.org/10.1175/JTECH-D-12-00089.1>, 2013.
 558 Maslanik, J., Stroeve, J., Fowler, C. and Emery, W.: Distribution and trends in Arctic sea ice age
 559 through spring 2011, *Geophys. Res. Lett.*, **38**, L13502, 2011.
 560 Mayer, M., Haimberger, L., Pietschnig, M. and Storto, A.: Facets of Arctic energy accumulation
 561 based on observations and reanalyses 2000-2015, *Geophys. Res. Lett.*, **43**, 10420-10429,
 562 2016.
 563 Screen, J.A. and Simmonds, I.: The central role of diminishing sea ice in recent Arctic temperature
 564 amplification, *Nature*, **464**, 1334-1337, 2010.
 565 Serreze, M.C., Holland, M.M. and Stroeve, J.: Perspectives on the Arctic’s shrinking sea ice cover,
 566 *Science*, **315**, 1533-1536, 2007.
 567 Smith, L.C. and Stephenson, S.R.: New Trans-Arctic shipping routes navigable by midcentury,
 568 *PNAS*, **110**, E1191–E1195, 2013.
 569 Uttal, T., Starkweather, S., Drummond, J.R., Vihma, T., Makshtas, A.P., Darby, L.S., Burkhart, J.F.,
 570 Cox, C.J., Schmeisser, L.N., Haiden, T., Maturilli, M., Shupe, M.D., de Boer, G., Saha, A.,
 571 Grachev, A.A., Crepinsek, S.M., Bruhwiler, L., Goodison, B., McArthur, B., Walden, V.P.,
 572 Dlugokencky, E.J., Persson, P.O.G., Lesins, G., Laurila, T., Ogren, J.A., Stone, R., Long, C.N.,
 573 Sharma, S., Massling, A., Turner, D.D., Stanitski, D.M., Asmi, E., Aurela, M., Skov, H.,
 574 Eleftheriadis, K., Virkkula, A., Platt, A., Førlund, E.J., Iijima, Y., Nielsen, I.E., Bergin, M.H.,
 575 Candlish, L., Zimov, N.S., Zimov, S.A., O’Neill, N.T., Fogal, P.F., Kivi, R., Konopleva-Akish, E.A.,
 576 Verlinde, J., Kustov, V.Y., Vasek, B., Ivakhov, V.M., Viisanen, Y., and Intrieri, J.M.: International
 577 Arctic Systems for Observing the Atmosphere: An International Polar Year Legacy
 578 Consortium. *Bull. Amer. Meteor. Soc.*, **97**, 1033–1056, [https://doi.org/10.1175/BAMS-D-14-](https://doi.org/10.1175/BAMS-D-14-00145.1)
 579 [00145.1](https://doi.org/10.1175/BAMS-D-14-00145.1), 2016.
 580
 581

Tables

Table 1: Known performance characteristics for TBS instruments. The asterisk with wind direction denotes that these stated specifications have not been met in the Arctic environment at Oliktok Point.

	Resolution	Accuracy	Range	Response Time
iMet-1-RSB				
Pressure [hPa]	< 0.01	+/- 0.5	2 - 1070	< 1 s
T [°C]	< 0.01	+/- 0.2	-95 to 50	2 s
RH [%]	< 0.1	+/- 5	0 - 100	2 s @ 25 °C
GPS Altitude [m, MSL]		+/- 15	0 – 30+ km	
GPS Position [deg]		+/- 10		
iMet XQ2				
Pressure [hPa]	0.01	+/- 1.5	10 - 1200	10 ms
T [°C]	0.01	+/- 0.3	-90 to 50	1 s @ 5 m/s flow
RH [%]	0.1	+/- 5	0 - 100	5.2 s @ 5 °C
APRS World Wind Vane				
Wind Speed [m s ⁻¹]	0.1	+/- 0.1 or 5% (whichever is greater)	1 - 59	
Wind Direction* [deg]	1	+/- 2	0 – 360	
POPS				
Particles Conc. [cm ⁻³]		+/- 10 % < 1000 cm ⁻³ at 0.1 LPM	0-1250 cm ⁻³	
CPC				
Particles Conc. [cm ⁻³]		+/- 2.5-3%	0-1E ⁴ cm ⁻³	
TBS Ground Station				
T [°C]	0.01	+/- 0.3	-95 to 50	< 1 s
RH [%]	0.1	+/- 2 @ 20 °C, < 90% RH, +/- 3 @ 20 °C, >= 90% RH +/- 0.3	0.8 - 100-95 to 50	15 s @ 20 °C < 1 s

Formatted: Font: 10 pt

Formatted: Font: 10 pt

Table 2: Known performance characteristics for DataHawk2 instruments. Note that accuracy estimates on wind values are estimated based on recent intercomparison with surface-based instrumentation, and apply to a higher-order derived product.

Data Type	Resolution	Accuracy	Range	Response Time
GPS position [deg]	0.010	+/- 10 m	-180 to 180 (lon), -90 to 90 (lat)	1s
GPS altitude [m, MSL]	0.010	+/- 10 m	-100 to 15000	1s
Baro pressure [mbar]	0.01	+/- 2.5	500 to 1030	0.022 s
Rel. humidity [%]	0.01	+/- 3	0 to 105	8 s
Slow temp. [°C]	0.015	+/- 2	-40 to 80	2 s
Coldwire Voltage [V]	0.0000078 [~0.025°C]	Unknown	-40 to +80 °C	0.5 ms @ 15 m/s
Airspeed [m/s]	0.01	0.2	0 to 30	0.3 ms
iMet, EE03, Temp [°C]	0.01	+/- 0.3 deg	-40 to + 85 deg C	1s
iMet, EE03, RH [%]	0.01	+/- 3%	0-95%	1s
wind <u>speed</u> [m/s]	0.01	+/- 1 m/s	0 to 100	0.1s
wind <u>direction</u> [deg]	0.01	+/- 15 deg	0 to 360	0.1s
<u>Vertical velocity</u> (m/s)	<u>0.01</u>	+/- 0.2 m/s	<u>-100 to 100</u>	<u>0.1s</u>

Deleted: degrees

Deleted: u

Deleted: Unknown

Deleted: -50 to 50

Deleted: v

Deleted: m/s

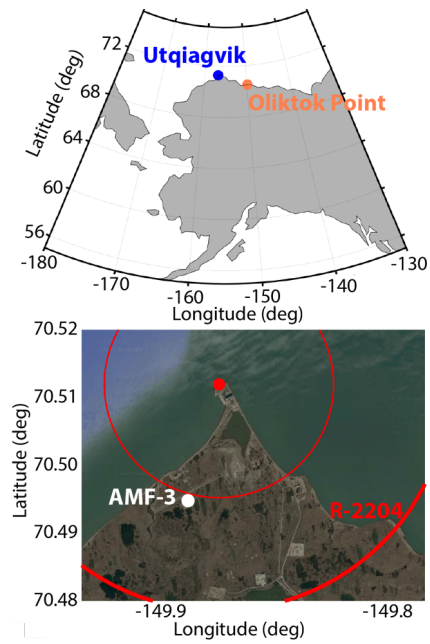
Deleted: Unknown

Deleted: -50 to 50

Deleted: wind_w [m/s]

... [1]

605 **Figures**
606



607
608 **Figure 1:** A map illustrating the location of Oliktok Point, Alaska (top). The lower panel is a
609 satellite image of the Oliktok Point area, including information on the boundaries of the R-2204
610 restricted airspace (bold red line), and the location of the DOE AMF-3 (white dot).
611

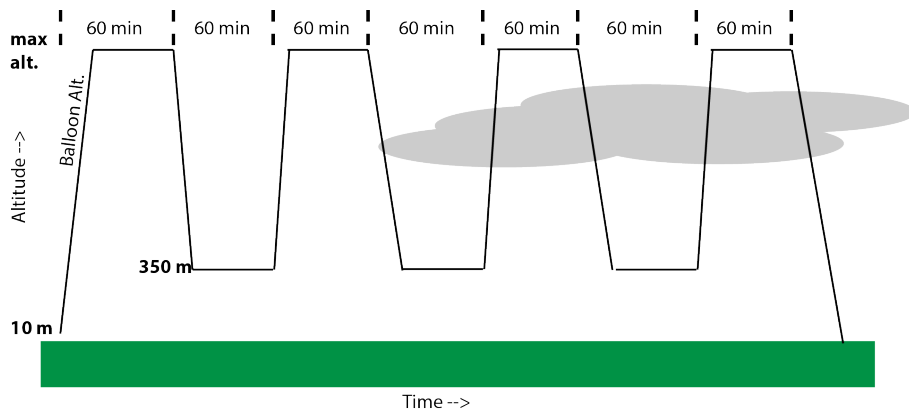


Figure 2: An illustration of the proposed TBS flight pattern for clear or cloudy conditions. The black lines are the proposed flight pattern, with time on the horizontal axis.

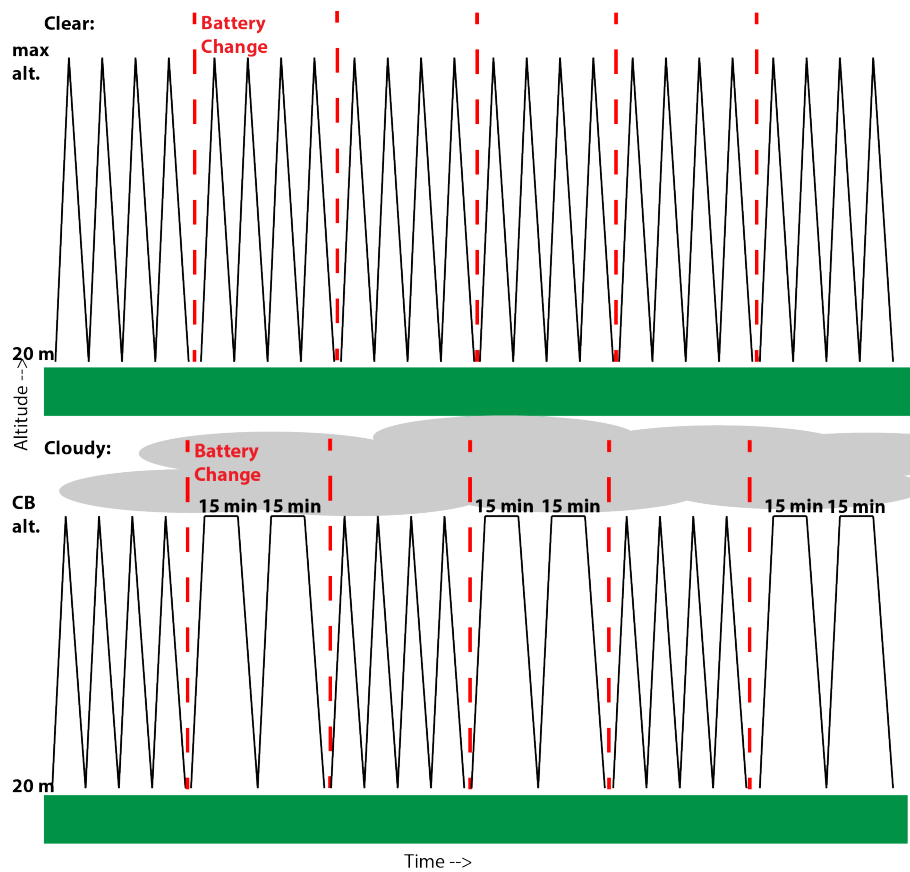
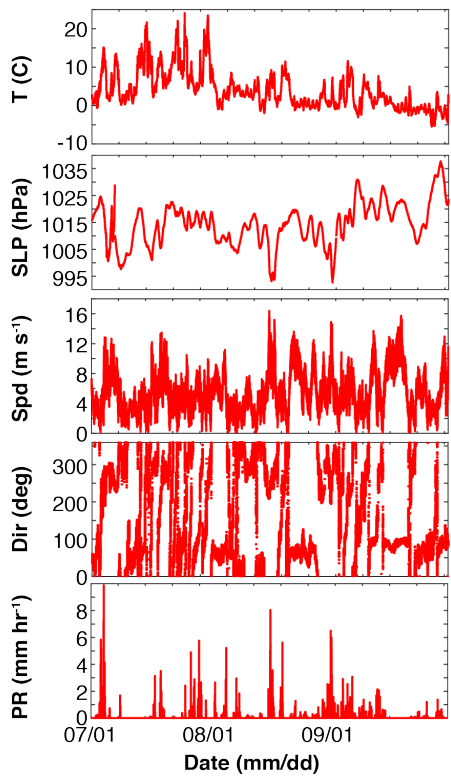


Figure 3: An illustration of the proposed DataHawk2 flight pattern for clear (top) and cloudy (bottom) conditions. The black lines are the proposed flight pattern on a time axis, while the red lines indicate battery changes in between flights.



621
622 **Figure 4:** Surface meteorological conditions (1-minute resolution), as measured by
623 instrumentation associated with the Oliktok Point AMF3 during POPEYE. From top to bottom
624 are: 2-meter air temperature, sea level pressure, 10-meter wind speed, 10-meter wind direction
625 and surface precipitation rate.
626

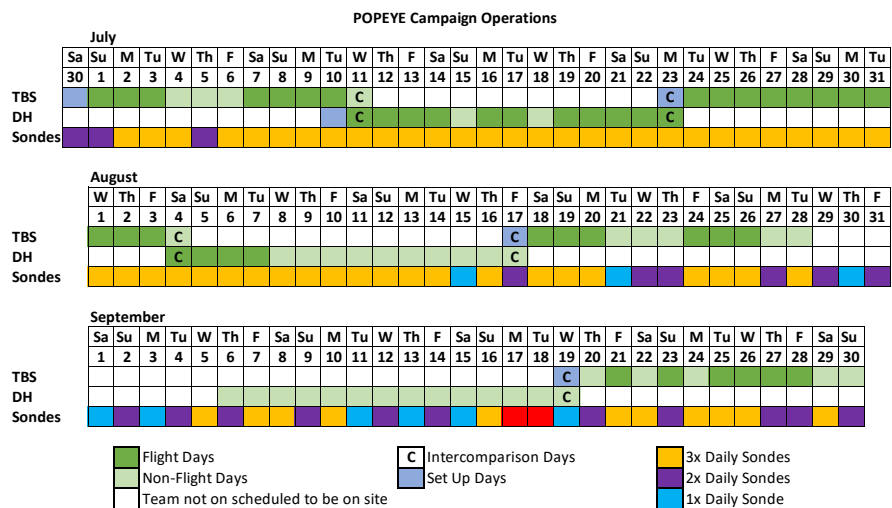


Figure 5: A graphical representation of actual UAS, TBS and radiosonde operations during POPEYE.

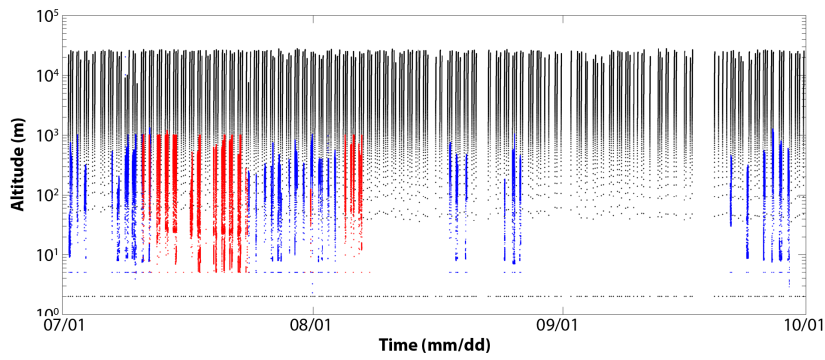


Figure 6: A time-height cross-section illustrating all of the POPEYE radiosonde launches (black dots), DataHawk2 flights (red dots) and tethered balloon flights (blue dots).

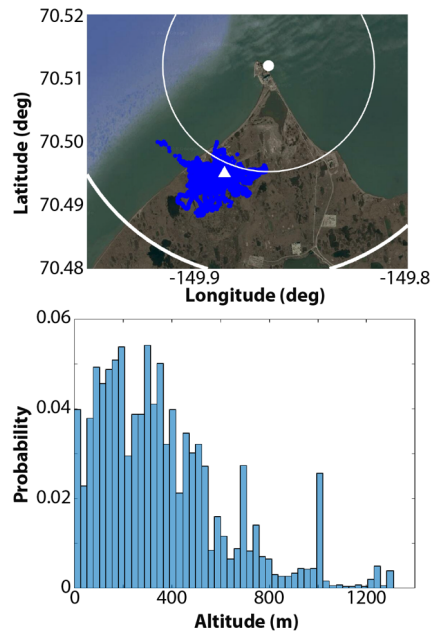
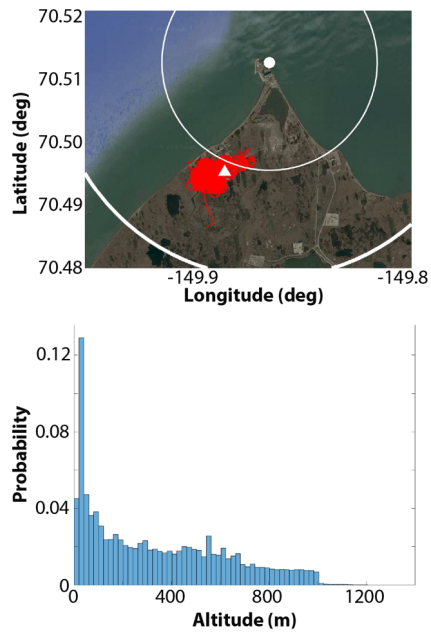
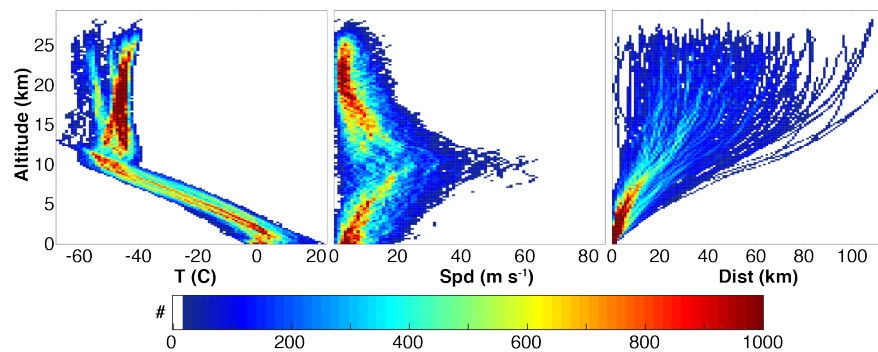


Figure 7: A spatial map of the POPEYE tethered balloon flight locations (top, blue dots), including white range rings at one and two nautical miles demonstrating the extent of R-2204 and the location of the AMF-3 (white triangle). The bottom panel is a relative frequency distribution of the altitudes sampled by the TBS during POPEYE.



642
643 **Figure 8:** A spatial map of the POPEYE DataHawk2 flight locations (top, red dots), including white
644 range rings at one and two nautical miles demonstrating the extent of R-2204 and the location
645 of the AMF-3 (white triangle). The bottom panel is a relative frequency distribution of the
646 altitudes sampled by the DataHawks during POPEYE.
647

648



649

650

Figure 9: Two-dimensional histograms of radiosonde temperature (left), wind speed (middle),
651 and distance from Oliktok Point (right), with altitude during POPEYE.

652

653

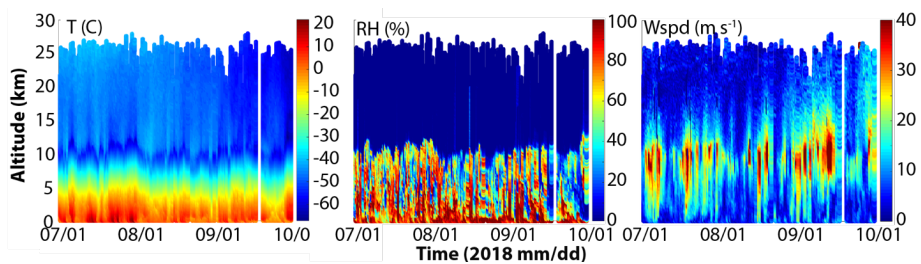


Figure 10: POPEYE radiosonde data, including time-height cross sections of (left to right) temperature, relative humidity and wind speed as observed during the second YOPP Special Observing Period.

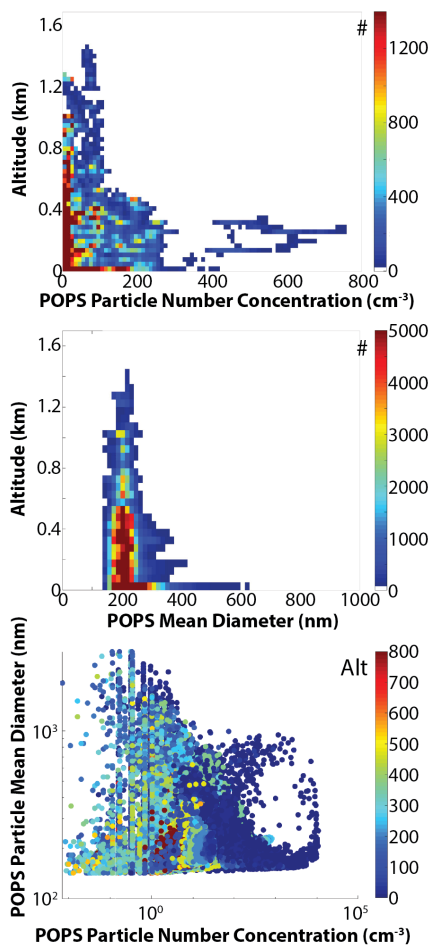


Figure 11: POPEYE aerosol statistics from the POPS sensor. Included are (top to bottom): a two-dimensional histogram of particle number concentrations sampled as a function of height; a two-dimensional histogram of the particle sized detected as a function of height; and a scatter plot showing the relationship between size and number, with colors representing altitude.

